11-10-1995

The Geometry and Kinematics of the Broad-Line Region in NGC 5548 from HST and IUE Observations

Ignaz Wanders
The Ohio State University

Mike R. Goad
Space Telescope Science Institute

Kirk T. Korista
University of Kentucky

Bradley M. Peterson
The Ohio State University

Keith Horne
University of St. Andrews, United Kingdom

See next page for additional authors

THE ASTROPHYSICAL JOURNAL, 453:L87–L90, 1995 November 10

THE GEOMETRY AND KINEMATICS OF THE BROAD-LINE REGION IN NGC 5548 FROM *HST* AND *IUE* OBSERVATIONS

IGNAZ WANDERS,[1] MIKE R. GOAD,[2] KIRK T. KORISTA,[3] BRADLEY M. PETERSON,[1] KEITH HORNE,[4] GARY J. FERLAND,[3] ANURADHA P. KORATKAR,[2] RICHARD W. POGGE,[1] AND JOSEPH C. SHIELDS[5,6]

Received 1995 July 11; accepted 1995 August 30

ABSTRACT

The spatial and radial velocity distribution of broad-line–emitting gas in the Seyfert 1 galaxy NGC 5548 is examined through the process of reverberation mapping, which is done by detailed comparison of continuum and emission-line variations. Recent spectroscopic monitoring of NGC 5548 with *HST* and *IUE* allows us to resolve the "transfer function" (TF) that relates the continuum and emission-line variability. We also examine the radial velocity–resolved TFs, and confirm that predominantly radial motions of the line-emitting clouds can be excluded. We find that a broad-line region comprised of clouds that are orbiting a central source of mass $\sim 10^8\ M_\odot$ along randomly inclined Keplerian orbits and irradiated by a beamed continuum source yields a TF and line profile that are qualitatively consistent with the observations. In this model, the clouds that produce the variable C IV emission lie within 12 lt-days of the central source, and the continuum radiation is confined to a wide biconical beam (semi–opening angle 35°–60°) with the observer viewing into the cone.

Subject headings: galaxies: active — galaxies: individual (NGC 5548) — quasars: emission lines

1. STRUCTURE OF THE BLR

During 1993, an intensive monitoring campaign of the active galactic nucleus (AGN) NGC 5548 was undertaken with the aim of obtaining the transfer function (TF) of the broad-line region (BLR). The TF (Blandford & McKee 1982; Peterson 1993) describes the distribution of time delays with which an emission line is observed to respond to changes in the ionizing continuum radiation. Assuming that the delays are due primarily to light-travel time within the BLR, the TF then provides information about the geometry, kinematics, and physical properties of the BLR.

Although a considerable amount of effort has gone into AGN monitoring in the past, the distribution and kinematics of the BLR material remains ill defined. Previous monitoring campaigns have shown that the BLR in NGC 5548 is very small, with the C IV emission line responding to continuum variations on timescales of a few days. Therefore, intensive monitoring with at least daily sampling and high signal-to-noise ratio (S/N) is required to resolve the TF on such short timescales. In 1993, *IUE* observations were made once every 2 days for a period of 75 days. During the last 39 days, *HST* Faint Object Spectrograph (FOS) spectra were obtained daily at nearly regular intervals. The raw data and their reduction are described in detail by Korista et al. (1995, hereafter K95).

K95 present a UV continuum light curve of combined *IUE* and *HST* data at 1350 Å (their Fig. 10), a total C IV emission-line light curve (their Fig. 8), and light curves of the blue wing (BW), blue core (BC), red core (RC), and red wing (RW) of the C IV line (their Fig. 9). K95 also present the cross-correlation functions (CCFs) of the C IV light curves with the UV continuum light curve (their Figs. 13 and 15), and they conclude that radial motions within the BLR are not predominant because of the nearly identical CCFs for the different velocity bins of the C IV line. In this Letter we go one step further, deconvolving the transfer equation of the BLR and deriving the TFs for the total C IV emission line, as well as for the BW, BC, RC, and RW components.

2. TRANSFER FUNCTIONS

We divided the C IV emission line into four velocity bins: a BW ($-10{,}000\ \mathrm{km\ s^{-1}} < v < -2450\ \mathrm{km\ s^{-1}}$), a BC ($-2450\ \mathrm{km\ s^{-1}} < v < 0\ \mathrm{km\ s^{-1}}$), an RC ($0\ \mathrm{km\ s^{-1}} < v < 2450\ \mathrm{km\ s^{-1}}$), and an RW ($2450\ \mathrm{km\ s^{-1}} < v < 10{,}000\ \mathrm{km\ s^{-1}}$), where v is measured relative to the emission-line center as defined by the peak of the narrow C IV line. These emission-line light curves differ only slightly from those presented by K95. Also, our CCFs are qualitatively very similar to theirs and do not differ significantly.

To derive the internal structure of the BLR, a cross-correlation analysis is insufficient and an inversion has to be done on the continuum and emission-line light curves [$C(t)$ and $L(v, t)$, respectively] to obtain the TF $\Psi(v, \tau)$: $L(v, t) = \int d\tau\ \Psi(v, \tau) C(t - \tau)$ (Blandford & McKee 1982). For the inversion of this equation we use both the SOLA method (Pijpers & Wanders 1994) and the maximum-entropy method (MEM; Horne 1994). In order to do a proper inversion, we need to calculate the TF to a maximum time delay τ of at least $\tau_{\max} = 2R_{\max}/c$, where $R_{\max}$ is the outer radius of the BLR and c is the speed of light.

Based on earlier studies, we know that the C IV TF falls to zero at about 30 days (Krolik et al. 1991), and hence the first 30 days of the line data will be discarded during the SOLA inversion process. The *HST* data alone cover too short a time span to recover the TF, and therefore we include the *IUE*

[1] Department of Astronomy, The Ohio State University, 174 West 18th Avenue, Columbus, OH 43210.
[2] Space Telescope Science Institute, 3700 San Martin Drive, Baltimore, MD 21218.
[3] Department of Physics and Astronomy, University of Kentucky, Lexington, KY 40506.
[4] University of St. Andrews, School of Physics and Astronomy, North Haugh, St. Andrews, Fife KY16 9SS, Scotland, UK.
[5] Steward Observatory, University of Arizona, Tucson, AZ 85721.
[6] Hubble Fellow.

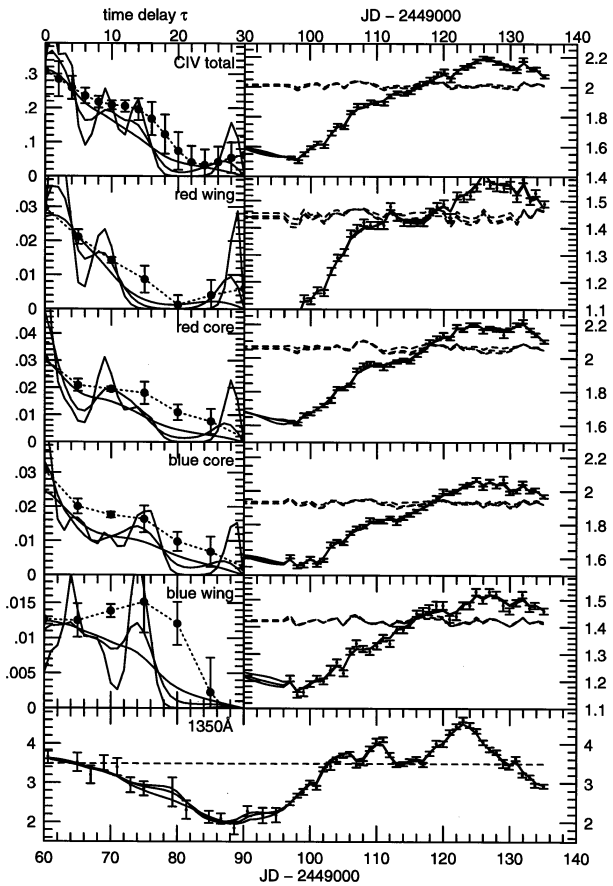

FIG. 1.—Recovered total-flux, BW, BC, RC, and RW TFs for C IV in NGC 5548. In the five left-hand panels the dots represent the SOLA TF solutions, while the solid lines show the MEM solutions. The five right-hand panels show the MEM reconstructed line light curves as solid lines and the background levels as dashed lines. The bottom panel depicts the MEM reconstructed continuum light curves and the background level. The three different MEM solutions correspond to $W = 0.1$, 1, and 10, with the smoothness of the TF solution increasing with W (Horne 1994).

continuum data in the analysis. In contrast, the *IUE* C IV emission-line data are not required.

We present the TFs for the four velocity intervals of the C IV emission-line profile in Figure 1 together with the total-flux TF of the C IV emission line. The TFs are shown in the five left-hand panels. The SOLA results are shown as large dots connected with dotted lines, and the MEM results are shown as solid lines. The control parameters used by SOLA were $\mu = 0.01$, $\tau_{max} = 40$ days, $N_s = 0$, and the resolution parameter $\Delta = 6$ days; thus the FWHM resolution of the SOLA TF is about 9 days. This is mainly due to the poorer temporal resolution and lower S/N of the *IUE* data. However, excluding the *IUE* data to improve the resolution is undesirable, as the extent of the *HST* time series alone is too short to recover the complete TF.

The five right-hand panels in Figure 1 show MEM fits to the emission-line data, and the lower panel shows MEM fits to the continuum-flux data (cf. Horne 1994). The three MEM solutions shown in Figure 1 differ in their "stiffness" parameter W, which was set to 0.1, 1, and 10 for these solutions, $W = 0.1$ having the highest resolution of the three. These MEM solutions achieve $\chi^2/N = 1$, but only by allowing the line background levels to vary as indicated in the five right-hand panels of Figure 1. These may be regarded as fits to residual photometric errors in the *HST* data, or as line variations that are not in response to the observed continuum variations. Note that the MEM and the SOLA method solve a slightly different transfer equation (responsivity- and emissivity-weighted TFs, respectively), and their amplitudes should not be compared directly (unless the lines respond strictly linearly to continuum variations). However, the time-delay information, i.e., the shape of the TF, is directly comparable.

It is found that within the limitations imposed by the flux uncertainties and time resolution, the MEM ($W \sim 1$–10) and SOLA solutions are largely consistent with each other. The BC and RC TFs are in good agreement and also show the main features of the total-flux TF: a monotonically declining function peaking at zero time lag with a superposed shoulder at a lag of ~10–14 days. This means that the TF is temporally resolved and has a finite width, since otherwise the SOLA-TF would have a Gaussian shape with a FWHM determined by the resolution of the inversion (i.e., FWHM ~ 9 days; Pijpers & Wanders 1994). However, the BW and the RW TFs are different: the RW TF lacks the 10–14 day shoulder of the total-flux TF, whereas the BW TF lacks the strong 0 day peak of the total-flux TF. This asymmetry is due to the more rapid rise of the RW flux at the beginning of the campaign. Done & Krolik (1995) interpret this feature as evidence for mild inflow.

An important result of this work is that *all* of the TFs show a significant response at zero lag. The present total-flux TF differs from the one derived by Krolik & Done (1995), but they used *IUE* data from 1989 (Clavel et al. 1991), which are not as well sampled and are much noisier than the data used here, and, hence, structure in the TF is not resolved. Also, the 1989 *IUE* light curve, which spans 8 months, is apparently nonstationary (Netzer & Maoz 1990), which makes the inversion prone to erroneous results.

3. A SIMPLE MODEL

A model for the BLR needs to take into account three characteristics of the TF:

1. There is significant emission-line response peaking at zero lag.
2. At a resolution of 9 days (FWHM), the TF decreases monotonically, with a shoulder at 10–14 days.
3. There are no strong differences in the positions of the centroids of the TFs and CCFs (K95) between the red and blue sides of the emission-line profile, hence radial motions are not predominant in the BLR.

Accretion disk and spherical-shell models for the BLR can explain these characteristics, but special conditions are needed for the radial distribution of the emissivity in the BLR in order to reproduce the shoulder. For example, a thick spherical shell could have enhanced emissivity at $R < 5$ days and 10 days $< R <$ 14 days, effectively being an inner region surrounded by a shell. A nearly edge-on disk with inner radius $R_{in} = 6$ lt-days produces a TF with a peak at 0 days and a shoulder at $2R_{in}/c = 12$ days (e.g., Fig. 5*a* of Welsh & Horne 1991). The edge-on aspect ($\cos i \approx H/R$) places material near the line of sight to produce the peak at 0 days, and the 12 day shoulder arises from the onset of response from the far side of the disk's inner rim. Alternatively, if R_{in} is very small (less than 3 days), then the 10–14 day shoulder could be response from the far side of the disk due to anisotropic C IV emission

(directed back toward the center). These disk models account for the observed TF, but they predict a double-peaked line profile with red and blue peaks shifted by the Keplerian velocity at the outer radius of the C IV region. This would need to be filled in by low-velocity emission.

We note that the shape of the TF, especially the presence of the shoulder, is a signature of a biconical BLR (Pérez, Robinson, & de la Fuente 1992; O'Brien, Goad, & Gondhalekar 1994, hereafter OB94). The near-side cone directed toward the observer produces the 0 day peak, and the far-side cone directed away produces the 10–14 day shoulder. A biconical BLR would imply radial flows in the BLR, contrary to the observations. However, a biconical BLR can be mimicked by biconical continuum radiation intersecting an otherwise spherical BLR. In this configuration, the total-flux TF will show the features of a bicone, while at the same time allowing the BLR material to move along randomly inclined Keplerian orbits, such that radial motions are not observed to be predominant. Provided that the near beam is directed toward the observer, this simple model can yield broad, single-peaked emission-line profiles very similar to the observed ones. We develop this model as an attractive, simple, and probably generalizable description of the geometry and kinematics of the BLR.

The parameters involved in the beamed-continuum model are the inner and outer radii ($R_{\rm in}$ and $R_{\rm max}$, respectively) of the spherical BLR, the radial-emissivity power-law index β (Goad, O'Brien, & Gondhalekar 1993), and the Keplerian velocity $v_{\rm K}$ at $R_{\rm in}$, and both the inclination i and semi–opening angle ω of the continuum beam. We will also take into account the possible importance of the anisotropy factor F, the fraction of line photons emerging from the irradiated face of the cloud (OB94; Ferland et al. 1992, who define an anisotropy factor $A = 2F - 1$), of the emission-line response.

For this model the inner radius of the BLR must be set to some small value in order to produce an unresolved peak in the TF at zero lag, and $R_{\rm in}$ is arbitrarily set to 1 lt-day in our model, although we could have chosen any value less than 3 lt-days. The outer radius is set by the lag $\tau_{\rm max}$ where the TF becomes zero: $R_{\rm max} = c\tau_{\rm max}/2 \approx 12$ lt-days. In order to produce an emission-line profile with the same FWHM as observed, the Keplerian velocity $v_{\rm K}$ at $R_{\rm in}$ is found to be 20,000 km s^{-1}. This then yields a mass M for the central object of almost $10^8\ M_\odot$. Since the line luminosity dependence is a strong function of radius [$L(r) \propto r^2$], C IV–emitting clouds in the inner regions of the BLR will be very difficult to detect observationally because they contribute so little to the total line emission.

Varying either β or F changes the relative importance of the shoulder with respect to the peak at zero lag. Models that are consistent with the deduced TF span a range in line anisotropy of $F \sim 0.5$–0.8 (OB94), which is also consistent with photoionization calculations for the C IV line (Ferland et al. 1992). The presently examined data can be well described by $F = 0.8$ and $\beta = -1$. Adopting these leaves us with the determination of i and ω. Model calculations show that if the observer is outside the beam (i.e., $\omega < i$), the emission-line profile is double-peaked. Because the observed emission-line profile is single-peaked (although we note that this may be hard to discern with a superposed narrow emission line; the narrow-line subtracted optical Hβ profiles of NGC 5548 [Wanders et al. 1995] are not double-peaked), we conclude that the observer is looking down the beam: $\omega > i$. A more complete calculation of profile shape as a function of inclination and semi–opening angle of the beam will be deferred to a future paper (Goad et al. 1995). The relative strength of the shoulder in the TF with respect to its peak at zero lag is also weakly dependent upon both i and ω; a narrow beam makes the velocity spread too narrow, while a wide beam makes the TF shoulder too weak. The model calculations yield a best qualitative fit if $i \approx 30°$ and $\omega \approx 45°$. We note, however, that a whole family of models with ω in the range $\sim 30°$–$60°$ are consistent with the data.

Figure 2 (Plate L7) shows a velocity-delay map for a representative beamed model that is qualitatively consistent with the observations. This is an idealized case, shown at arbitrarily high time resolution, and is built using the aforementioned parameter settings. The gray-scale plot shows the velocity-dependent TF, the bottom panel shows the delay-time integral of the TF (i.e., the time-averaged variable line profile), and the right-hand panel shows the total-flux TF. The model predicts that the BC and RC TFs peak at zero time delay and have a shoulder at larger lag, whereas both the RW and BW TFs are expected to peak away from zero (or to be rather flat at low resolution) and have a shoulder at larger lag (which, in low resolution, merges with the peak at smaller lag to produce the extended plateau).

Degrading the resolution of the model TF to match the 9 day FWHM of the observed TF, and integrating over the BW, BC, RC, and RW velocity ranges, yield model TFs that are directly comparable to those recovered from the observations. These are presented in Figure 3. They are qualitatively very similar to the observed TFs from Figure 1. Figure 3 also compares the predicted and observed (K95) velocity profiles.

We note that our model is consistent with the independently derived inclination, $i \approx 20°$–$30°$, for the purported accretion disk in NGC 5548 from X-ray observations of the broad Fe Kα line (Mushotzky et al. 1995). Interestingly, Wilson & Tsvetanov (1994) show that most of the 11 known Seyfert galaxies with biconical extended narrow-line regions have semi–opening angles in the range $30°$–$60°$, similar to the range we find for ω in NGC 5548. During the final stages of this work, we became aware of the fact that D. Axon and A. Robinson (1995, private communication) similarly advocate continuum beaming as an explanation for C IV profile variations in NGC 3516.

Our best-fit model can be regarded as a simplified version of the more general case for which the beam strength decreases with increasing semi–opening angle, as might be expected for a continuum originating from an accretion disk (Netzer 1987). Thence, the beam in our model is a weighted average of the continuum flux over the angular distribution and is to be regarded as an "effective" beam. We expect BLR material to lie outside the beam, and it is conceivable that a more isotropic continuum component dominates the photoionization of this gas. The line-emitting clouds which see this component will have a TF peaking at or near $\tau = 0$ depending on the line anisotropy, falling off monotonically after $\tau = 2R_{\rm in}/c$ (Blandford & McKee 1982). The small $R_{\rm in}$ implied by the model suggests that we cannot at present resolve the structure of the TF on these short timescales. However, its effect will be to increase the height of the central peak of the model TFs shown in Figure 3. The observed TFs certainly suggest that a more isotropic component is present.

As our model calculations show (Goad et al. 1995), the farther away the observer is from the beam axis, the more double-peaked the emission-line profiles become. At the same time, as the inclination increases the observed continuum will

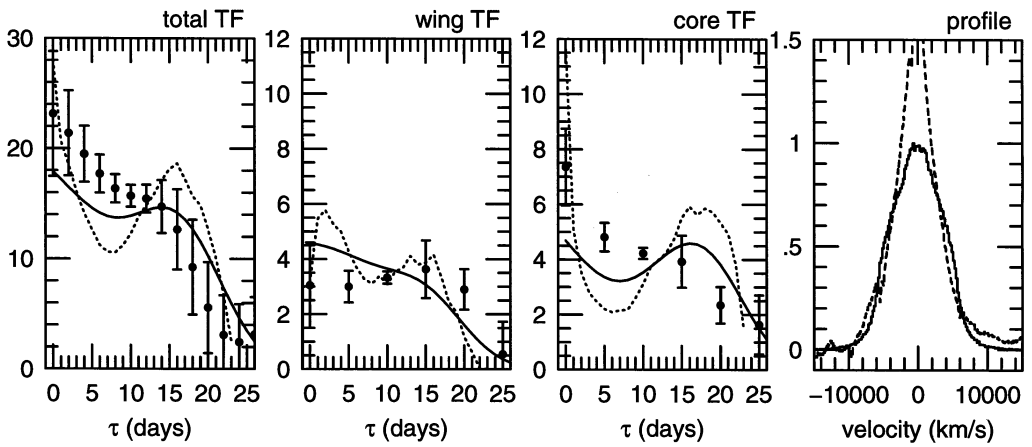

FIG. 3.—Model and observed TFs for the C IV total-flux, wing, and core components. The dashed lines represent the model TFs at full resolution, while solid lines show the same TFs at the reduced resolution provided by the observational measurements. The dots represent the total-flux, BW, and BC SOLA solutions from Fig. 1. Also shown are the model time-averaged variable profile from Fig. 2 (*solid line*) and the observed average line profile from K95 (*dashed line*).

become weaker, whereas the total strength of the emission lines will be unaffected. Hence, a prediction of this model is that, on average, double-peaked profiles should have larger equivalent widths than single-peaked profiles.

4. CONCLUSIONS

To summarize our results, we have derived and presented the C IV transfer function of the Seyfert 1 galaxy NGC 5548, observed by *HST* during a monitoring campaign in 1993. The TF shows resolved structure in the form of a shoulder on an otherwise monotonically declining function peaking at zero lag.

Although disk and spherical models may also be consistent with the data, we present an alternative, testable model for the C IV–emitting region in which the anisotropy of the continuum source plays a significant role. This model consists of emitting material on randomly inclined Keplerian orbits, spherically distributed around the central continuum source, and irradiated by a *beamed* continuum flux. The outer radius of the C IV–emitting region is found to be ~12 lt-days, and the inner radius less than about 5 lt-days. The semi–opening angle of the beam is between approximately 30° and 60°, and the observer is inside the beam. The mass of the central black hole is estimated to be almost $10^8\ M_\odot$.

This simple model may be regarded as a unification model for the BLR, such that the diversity among the line profiles of different AGNs (Robinson 1995) might be due to differences in inclination of the system. The model thus predicts that double-peaked profiles have larger equivalent widths on average than single-peaked profiles.

We thank Matt Malkan for helpful comments. We wish to thank Frank Pijpers for supplying the SOLA code used here. We gratefully acknowledge support for this work by NASA through grants NAG5-2477 and NAGW-3315 and through grants GO-3484.01-91A and AR-5280.01-93A from the Space Telescope Science Institute, which is operated by the Association of Universities for Research in Astronomy, Inc., under NASA contract NAS5-26555. I. W. acknowledges support from The Ohio State University through a University Fellowship. M. R. G. thanks The Ohio State University, and M. R. G. and I. W. thank the University of Kentucky for hospitality during part of this work.

REFERENCES

Blandford, R. D., & McKee, C. F. 1982, ApJ, 255, 419
Clavel, J., et al. 1991, ApJ, 366, 64
Done, C., & Krolik, J. H. 1995, ApJ, submitted
Ferland, G. J., Peterson, B. M., Horne, K., Welsh, W. F., & Nahar, S. N. 1992, ApJ, 387, 95
Goad, M. R., O'Brien, P. T., & Gondhalekar, P. M. 1993, MNRAS, 263, 149
Goad, M. R., et al. 1995, in preparation
Horne, K. 1994, in ASP Conf. Ser. 69, Reverberation Mapping of the BLR in AGNs, ed. P. M. Gondhalekar, K. Horne, & B. M. Peterson (San Francisco: ASP), 23
Korista, K. T., et al. 1995, ApJS, 97, 285 (K95)
Krolik, J. H., & Done, C. 1995, ApJ, 440, 166
Krolik, J. H., Horne, K., Kallman, T. R., Malkan, M. A., Edelson, R. A., & Kriss, G. A. 1991, ApJ, 371, 541
Mushotzky, R. F., Fabian, A. C., Iwasawa, K., Kunieda, H., Matsuoka, M., Nandra, K., & Tanaka, Y. 1995, MNRAS, 272, L9
Netzer, H. 1987, MNRAS, 225, 55
Netzer, H., & Maoz, D. 1990, ApJ, 365, L5
O'Brien, P. T., Goad, M. R., & Gondhalekar, P. M. 1994, MNRAS, 268, 845 (OB94)
Pérez, E., Robinson, A., & de la Fuente, L. 1992, MNRAS, 256, 103
Peterson, B. M. 1993, PASP, 105, 247
Pijpers, F. P., & Wanders, I. 1994, MNRAS, 271, 183
Robinson, A. 1995, MNRAS, 272, 647
Wanders, I., et al. 1995, in preparation
Welsh, W. F., & Horne, K. 1991, ApJ, 379, 586
Wilson, A. S., & Tsvetanov, Z. I. 1994, AJ, 107, 1227

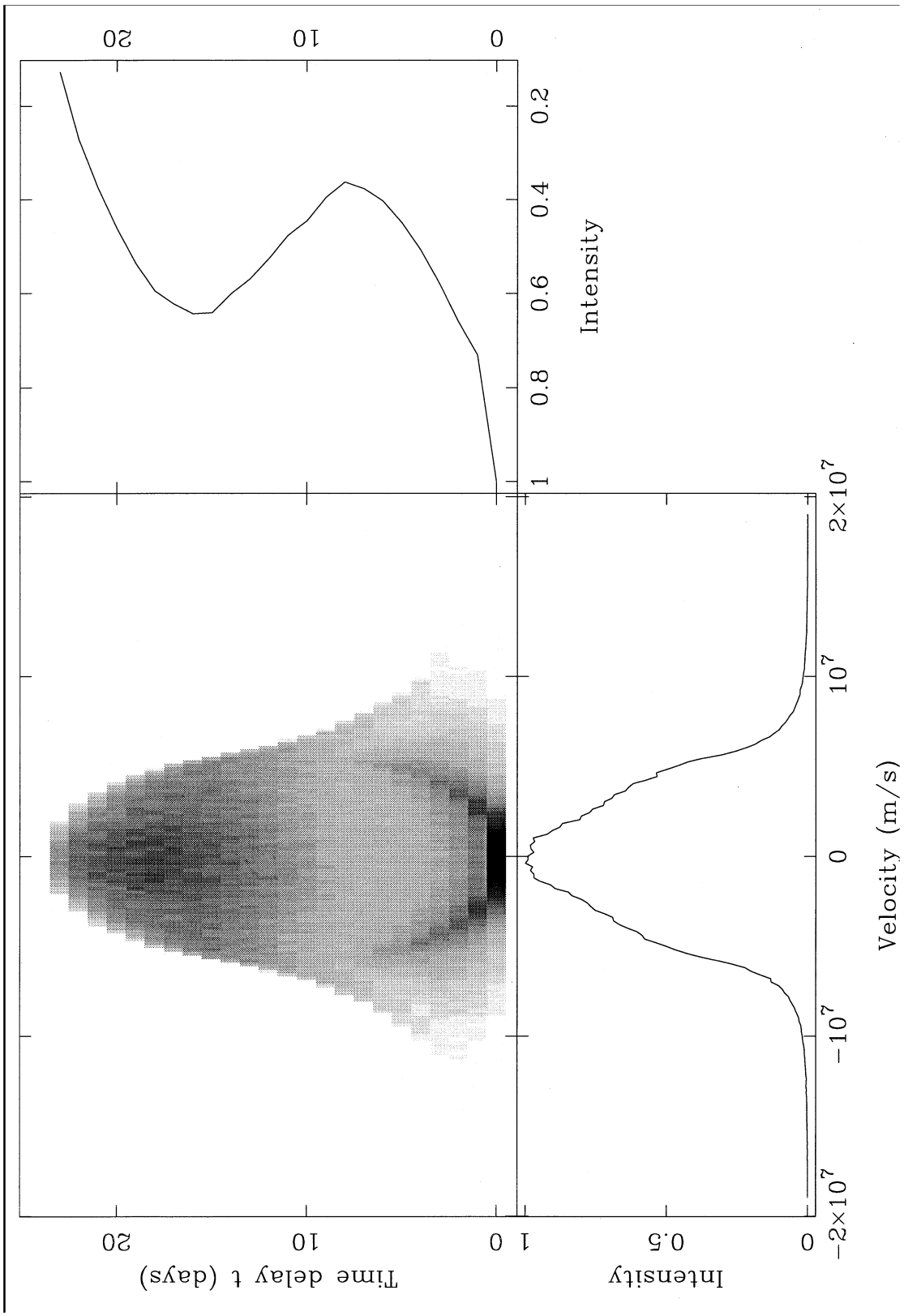

FIG. 2.—Representative model for the variable BLR consisting of a spherical distribution of optically thick clouds ($F = 0.8$) moving along randomly inclined Keplerian orbits, irradiated by a beamed continuum source. *Upper left-hand panel:* two-dimensional TF; *right-hand panel:* total-flux TF; *bottom panel:* time-averaged variable profile.